On dynamic models of flotation with sedimentation

R. Bürger*, S. Diehl, M. C. Martí***, Y. Vásquez***

* CI^{2}MA and Departamento de Ingeniería Matemática, Universidad de Concepción, Casilla 160-C, Concepción, Chile, rburger@ing-mat.udec.cl, yvasquez@ci2ma.udec.cl
** Centre for Mathematical Sciences, Lund University, P.O. Box 118, S-221 00 Lund, Sweden, stefan.diehl@math.lth.se
** Departament de Matemàtiques, Universitat de València, Avda. Vicent Andrés Estellés s/n, Burjassot, València, Spain, Maria.C.Marti@uv.es

Abstract: Flotation is a separation process where particles or droplets are removed from a suspension with the aid of floating gas bubbles. One application is dissolved air flotation in industrial wastewater treatment. One-dimensional models of flotation have been confined to steady-state situations for half a century by means of the drift-flux theory. A new dynamic model with partial differential equations is used which also includes the simultaneous settling of particles that are not attached to bubbles. Optimal steady-state operating conditions can be chosen by means of operating charts. Responses to control actions are exemplified by simulations with a new numerical method.

Keywords: dissolved air flotation, settling, separation, multiphase flow, partial differential equation

Introduction

Gas flotation is a process to separate particles or droplets from a suspension when the particles/droplets are either too small or have a density close to that of water to settle efficiently. The gas bubbles and particles/droplets form aggregates which rise to the top of a flotation tank where a layer of froth is skimmed off; see Figures 1 and 2 for two applications. The suspension may also contain hydrophilic particles that do not attach to bubbles and settle to the bottom where they are removed in the underflow.

The flotation process is commonly used in industrial wastewater treatment to remove contaminants that are difficult to separate by other means such as floating solids, residual chemicals, droplets of oil and fat, and in mineral processing to recover valuable minerals (Finch and Dobby, 1990; Rubio *et al*., 2002; Wang *et al*., 2007). For oil-water separation in wastewater treatment, there exist several induced and dissolved air flotation (DAF) technologies (Saththasivam *et al*., 2016). DAF has been used for many years for the thickening of waste activated sludge (WAS) (Katz and Geinopolos, 1967; Butler *et al*., 1997; Chung and Kim, 1997; Haarhoff and Bezuidenhout, 1999). One of many advantages is that DAF can thicken sludge to concentrations at least two times higher than gravity settling (Wang *et al*., 2007; Reali *et al*., 2014). The flotation process is used for separating out either valuable or unwanted material at the top.

In mineral processing, the valuable minerals are made hydrophobic, attach to the bubbles and thereby form rising aggregates, while the hydrophilic gangue settles and is removed as tailings in the underflow (Finch and Dobby, 1990); see Figure 1. In the process of DAF thickening, simultaneous flotation of WAS and sedimentation of grit and other substances may occur (Butler *et al*., 1997; Wang *et al*., 2007); see Figure 2. Small air bubbles are trapped with the larger WAS flocs, which then float. In other applications, very small hydrophobic oil droplets attach to the air bubbles, while the grit settles. The simultaneous flotation-sedimentation process means that three phases are involved: liquid, buoyant aggregates and settling solids. We present results from ongoing research (Bürger *et al*., 2018, 2019) on general dynamic models for this three-phase process.

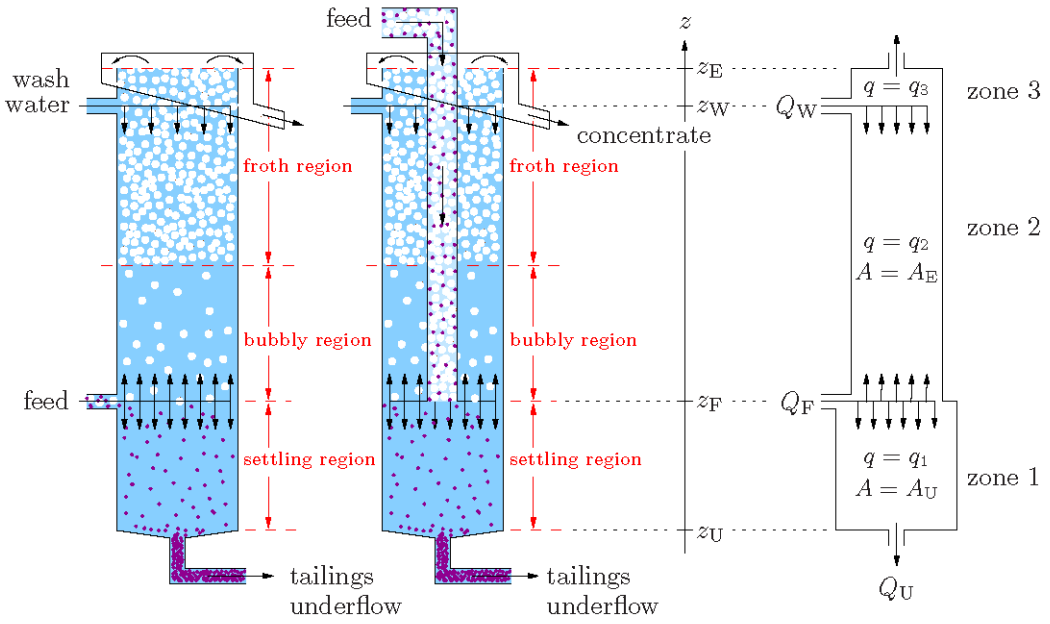

Figure 1 (From Bürger *et al*., 2019.) Schematic of a flotation column with a feed inlet for slurry mixture and gas. At the top, wash water can be injected for desliming of unwanted particles. In the Reflux Flotation Cell (Dickinson and Galvin, 2014), the fluid-gas-particle slurry is feed through a downcomer pipe, which makes the cross-sectional area vary with the height z. We use the values $A_E = 72.25$ cm^2 and $A_U = 83.65$ cm^2, and consider a laboratory scale column of height 1 m with $z_F = 33$ cm and $z_W = 90$ cm. The bulk velocities are $q_1 = -Q_U/A$, $q_2 = (-Q_U + Q_F)/A$ and $q_3 = (-Q_U + Q_F + Q_W)/A$.

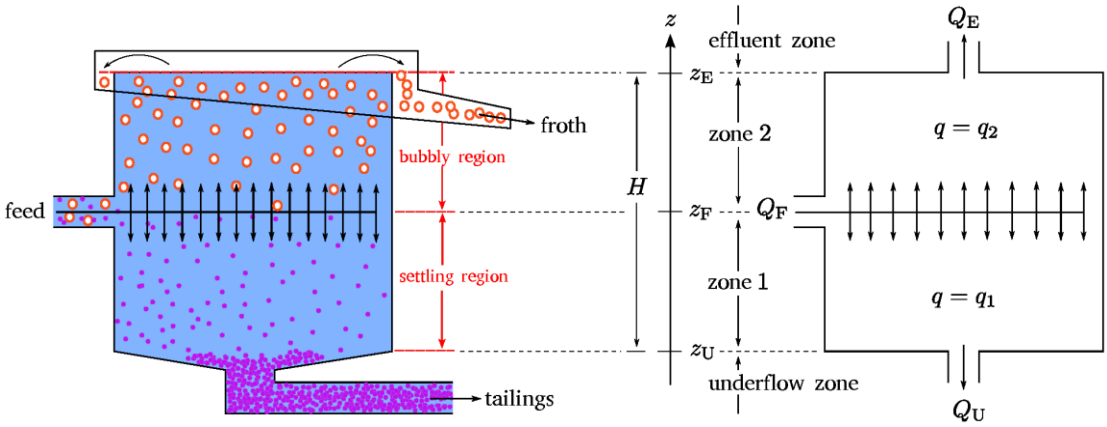

Figure 2 Schematic of a DAF thickener (cf. Wang *et al*., 2007) with constant cross-sectional area $A = \pi\, 2.5^2$ m^2 $= 19.635$ m^2, height $H = 2$ m and feed inlet at $z_F = 1$ m.

One-dimensional (1D) models of flotation columns for the two-phase flow of aggregates and fluid have been based on the drift-flux theory (Wallis, 1969; Dickinson and Galvin, 2014), or empirical relationships (Bratby and Ambrose, 1995), which can model steady state situations only. The rise of aggregates in a fluid, described by a batch drift-flux function, is conceptually similar to the settling of particles described by a batch settling-flux function. Contrary to the case of flotation, widely accepted dynamic 1D simulation models for continuous sedimentation based on partial differential equations (PDEs) have been developed since the 1990s (Bürger *et al*., 2013).

The purpose of this contribution is to demonstrate that a new three-phase flow PDE model by Bürger *et al*. (2019) for 1D modelling of simultaneous flotation and sedimentation can be utilized for different flotation applications. In particular, we present a new *operating chart* for the control of steady-states of DAF thickening with sedimentation (Figure 6). The designs of flotation columns and DAF tanks are variable

and since the purpose here is to advance a conceptual general model, we use the tank dimensions shown in Figures 1 and 2, and drift and settling flux functions in agreement with literature on column flotation by Dickinson and Galvin (2014) and Galvin and Dickinson (2014).

For the numerical simulations, we employ a newly developed numerical method (Bürger *et al*., 2019) for the PDE system that has been adapted from a general treatment by Karlsen *et al*. (2009).

Methods

We assume that all aggregation of (hydrophobic) particles and bubbles occurs before the slurry is fed into the column; e.g. in the incoming pipes. Figure 1 shows a typical vessel for froth flotation, where wash water can be injected at the top, while Figure 2 shows a DAF thickener which has no wash water. The conservation of mass for the three phases of aggregates, fluid and (hydrophilic) solids can be used to derive the following system of PDEs (Bürger *et al*., 2019):

$$\frac{\partial(A(z)\phi)}{\partial t} + \frac{\partial(A(z)J(\phi,z,t))}{\partial z} = Q_{\mathrm{F}}\phi_{\mathrm{F}}\delta(z-z_{\mathrm{F}}), \tag{1}$$

$$\frac{\partial(A(z)(1-\phi)\varphi)}{\partial t} - \frac{\partial(A(z)F(\varphi,\phi,z,t))}{\partial z} = Q_{\mathrm{F}}\phi_{\mathrm{s,F}}\delta(z-z_{\mathrm{F}}). \tag{2}$$

The unknowns ϕ and φ depend on height z and time t. The volume fraction of aggregates is ϕ and solids ϕ_{s}. The variable $\varphi = \phi_{\mathrm{s}}/(1-\phi)$ is the volume fraction of (hydrophilic) solids within the suspension. The total flux functions $J(\phi,z,t)$ and $F(\varphi,\phi,z,t)$ for the rising aggregates and the settling solids, respectively, contain the batch drift-flux and settling-flux functions, and the zone bulk velocities q_k, $k = 1,2,3$, which depend on the inlet volumetric flows Q_{F} and Q_{W} and the cross-sectional area $A(z)$. The delta functions on the right-hand sides model the feed inlet at $z = z_{\mathrm{F}}$, where ϕ_{F} and $\phi_{\mathrm{s,F}}$ are the volume fractions of aggregates and solids, respectively. We refer to Bürger *et al*. (2019) for exact definitions and all details of the numerical method.

The batch drift-flux function $j_{\mathrm{b}}(\phi)$ for the rising aggregates and the batch settling-flux function $f_{\mathrm{b}}(\varphi)$ for the solids have the same principle concave-convex form with one inflection point. The choice of function (polynomial, exponential, power law, etc.) for $j_{\mathrm{b}}(\phi)$ and $f_{\mathrm{b}}(\varphi)$ depends on the materials and belongs to the model calibration step. The choice does not influence the qualitative behaviour of the process. In fact, it is the purpose of this contribution to provide insight to the qualitative behaviour of the process; specific numerical values are of minor interest. For the rising aggregates we use the following batch drift-flux function:

$$j_{\mathrm{b}}(\phi) = \phi v_{\mathrm{term}}(1-\phi)^n, \tag{3}$$

where the terminal velocity of a single bubble water is $v_{\mathrm{term}} = 2.7$ cm/s and the dimensionless parameter $n = 3.2$ (Dickinson and Galvin, 2014). For $f_{\mathrm{b}}(\varphi)$, the same expression (3) is commonly used and we have chosen $v_{\mathrm{term,s}} = 0.5$ cm/s and $n_{\mathrm{s}} = 2.5$, which means that a single hydrophilic particle settles slower than an aggregate rises. In the present model, we neglect compression effects at high concentrations.

The PDE (1) contains only the unknown ϕ and this equation was analysed by Bürger *et al*. (2018). The analysis of the PDE system here, which includes the settling of hydrophobic particles, is more involved; however, once Equation (1) is solved for $\phi = \phi(z,t)$ for a certain time period, Equation (2) can in principle be solved for φ as a scalar

equation with $\phi(z,t)$ as a known function. We utilize this in the numerical method and in the classification of desired steady states.

The analysis of the stationary solutions of (1) and (2) is involved and needs a so-called entropy condition (Diehl, 1996) to obtain the physically correct solutions of the PDE system. Assume that feed volume fractions ϕ_{F} and $\phi_{\mathrm{s,F}}$ are given. There are several nonlinear conditions that have to be satisfied for a certain steady state to exist because of the feed inlets and discontinuities of the solution. The local maxima and minima of the zone flux functions are involved and we refer to Bürger *et al*. (2019) for all details. The nonlinear conditions can be visualized in operating charts (cf. Figures 3 and 6), where an operating point $(Q_{\mathrm{F}}, Q_{\mathrm{U}})$ in the white region means that all conditions are satisfied. For column flotation with wash water, the value of Q_{W} is calculated from a mass balance equation involving the two inlets. An operating chart depends on the feed inputs ϕ_{F} and $\phi_{\mathrm{s,F}}$ as can be seen in Figure 3. We emphasize that the conditions for obtaining a certain steady state are only necessary; the actual state depends also on the dynamic history of the process. This is demonstrated in the next example.

Column froth flotation with wash water

Two operating charts for flotation in mineral processing are shown in Figure 3 for a desired steady-state solution having a layer of froth in zone 3, a possible froth discontinuity in zone 2, and solids only in zone 1 (Bürger *et al*., 2019: case SS31). In the operating chart in Figure 3 (right), which is valid for $\phi_{\mathrm{F}} = 0.4$ and $\phi_{\mathrm{s,F}} = 0.2$, we choose the operating point $(Q_{\mathrm{U}}, Q_{\mathrm{F}}) = (40, 50)$ cm^3/s in the white region; see the blue asterisk. The wash water volumetric flow is calculated to $Q_{\mathrm{W}} = 14.46$ cm^3/s, which is the maximum that can flow downwards through the foam. A larger value would give overflow of wash water through the effluent.

Figures 4 and 5 show a simulation when the column is initially filled with only fluid. Very quickly a steady state is reached at $t = 180$ s; see Figures 4 (left) and 5(a). This has a low concentration of aggregates at the top and we perform some control actions.

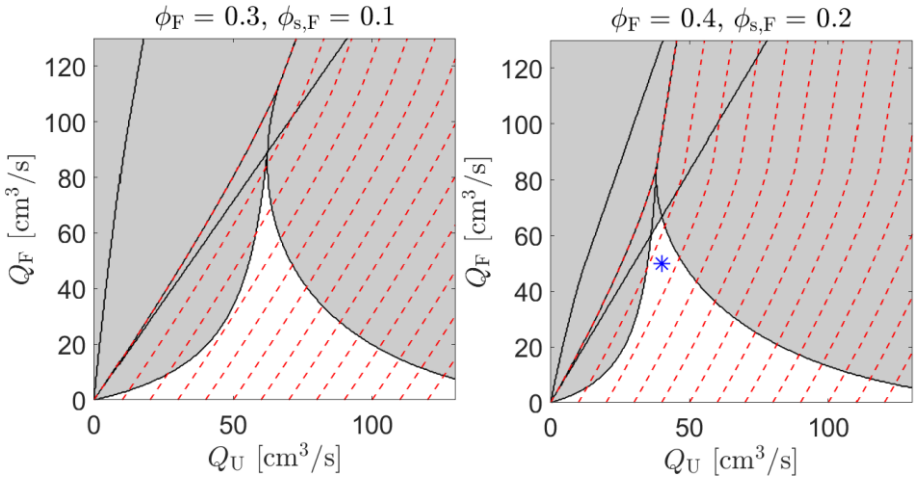

Figure 3 Column froth flotation: Examples of operating charts showing the intersection of several nonlinear inequalities for given feed volume fractions of aggregates ϕ_{F} and solids $\phi_{\mathrm{s,F}}$. The white region shows what values of $(Q_{\mathrm{U}}, Q_{\mathrm{F}})$ that can be chosen to obtain a desired steady state. The top corner of the white region gives the maximum possible value for Q_{F} which is the optimal handling capacity. Along each red dashed curve the volumetric wash water flow Q_{W} is constant and its value can be read off on the Q_{U}-axis. That is, on the leftmost curve $Q_{\mathrm{W}} = 0$ cm^3/s, on the next one $Q_{\mathrm{W}} = 10$ cm^3/s, etc.

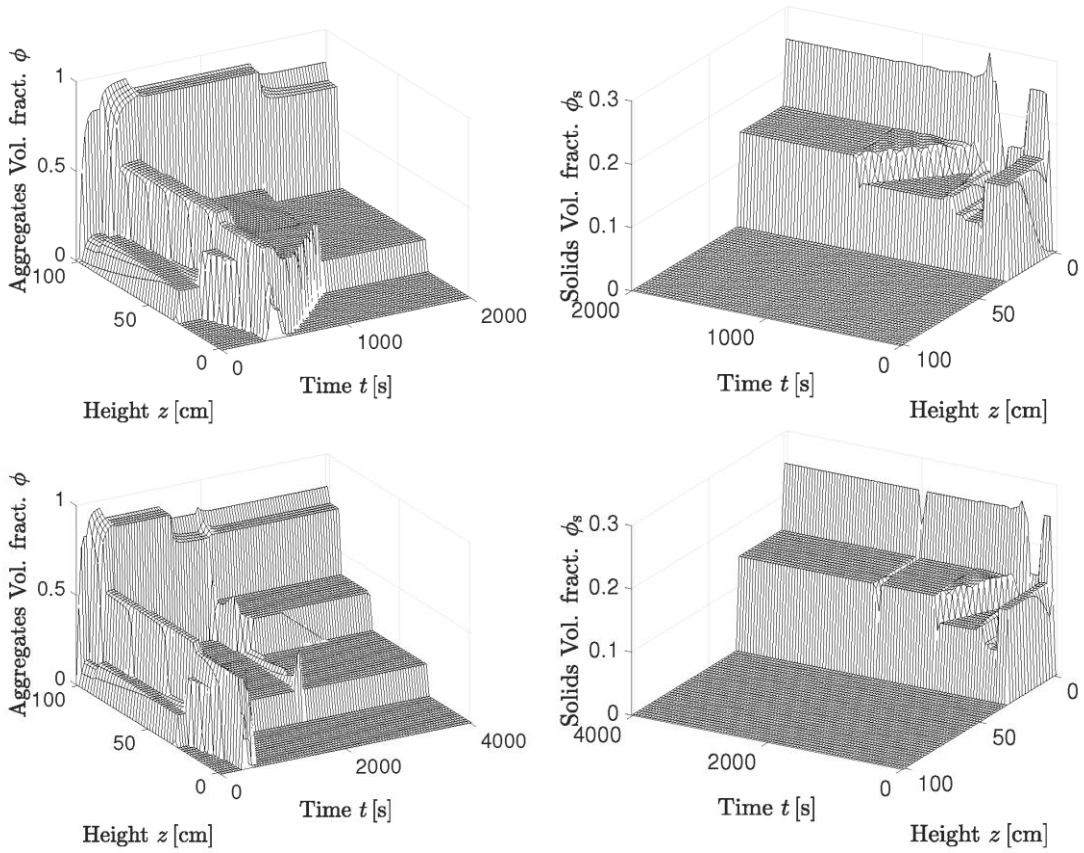

Figure 4 Simulation of a flotation column with volume fractions of aggregates (left) and solids (right) as functions of height z [cm] and time t [s]. The upper row show the first 2000 seconds and the lower row the entire simulation to $t = 4000$ s.

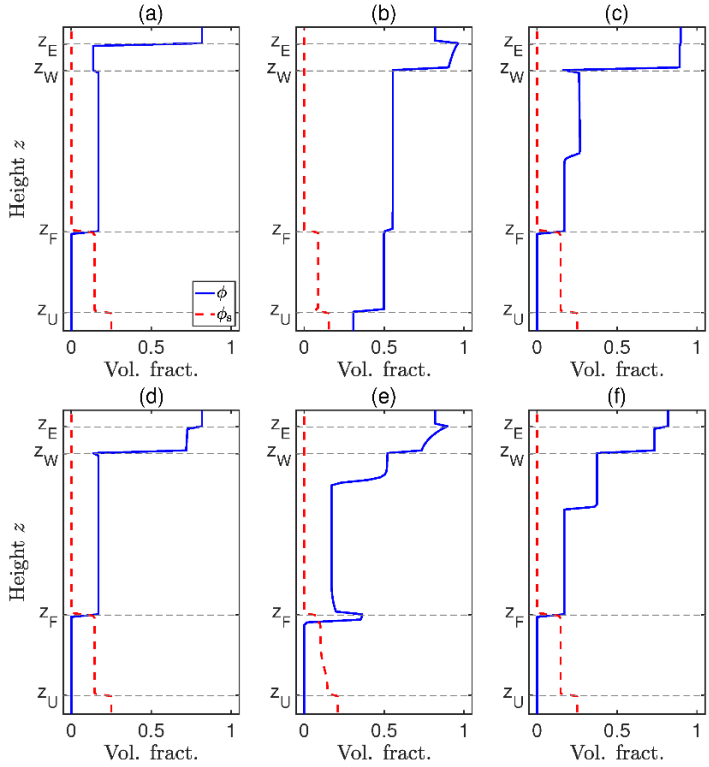

Figure 5 Snapshots of the simulation shown in Figure 4 at $t = 180$, 420, 1300, 2000, 2020 and 4000 s for the volume fractions of the aggregates ϕ_F (solid blue) and solids $\phi_{s,F}$ (dashed red).

At $t = 180$ s, the top is closed until $t = 420$ s by temporarily setting $Q_U = 64.46$ cm^3/s (so that the effluent volumetric flow is $Q_E = 0$ cm^3/s). Aggregates will then fill out the column and leave at the underflow with the volume fraction $\phi_U = 0.3$. After $t = 420$ s, the aggregates move upwards and at about $t = 2000$ s a steady state is reached (see Figure 5d). A high concentration of froth can only be found in the small zone 3. During 20 s, we close the top again, which eventually gives a new steady state at about $t = 4000$ s with a high froth concentration also in the upper part of zone 2, which is a desired steady state in mineral processing.

DAF thickening with sedimentation

A DAF thickener is shown in Figure 2. For simplicity we assume that the cross-sectional area is constant. Since there is no wash water, the fluid flow in zone 2 above the feed inlet is upwards. This constraint can be written as the inequality

$$Q_F - Q_U - Q_F \phi_F > 0 \tag{4}$$

and for given ϕ_F this means an (upper left) triangular region in the operating chart; see two such in Figure 6. For the derivation of condition (4), we refer to Bürger *et al.* (2019); see condition (FIIIa) therein. Condition (4) implies that the effluent volumetric flow $Q_E = Q_F - Q_U > 0$. The other curves that define the white region in the operating chart originate from two nonlinear inequalities involving $j_b(\phi)$ and one involving $f_b(\varphi)$ (Bürger *et al.*, 2019: conditions (FIa), (FIb) and (FIas)). These four conditions are necessary for having a steady state in the DAF thickener where aggregates are only present above the feed level and solids only below.

We perform a simulation where the DAF tank is initially only filled with water and $\phi_F = 0.2$ and $\phi_{F,s} = 0.2$. With the operating point $(Q_U, Q_F) = (300, 450)$ m^2/h in the white region of Figure 6 (left), the simulation is shown in Figure 7. A first steady state arises quickly after about $t = 0.07$ h $= 4.2$ min. Then we change the feed volume fraction of aggregates to $\phi_F = 0.4$ and simulate the reaction of the system; see Figure 7(a, b). As Figure 7(a) shows, aggregates accumulate at the top of the vessel and a growing layer reaches and passes below the feed point. In the corresponding operating chart for this new set of variables, Figure 6 (right), the blue operating point lies outside the admissible white region.

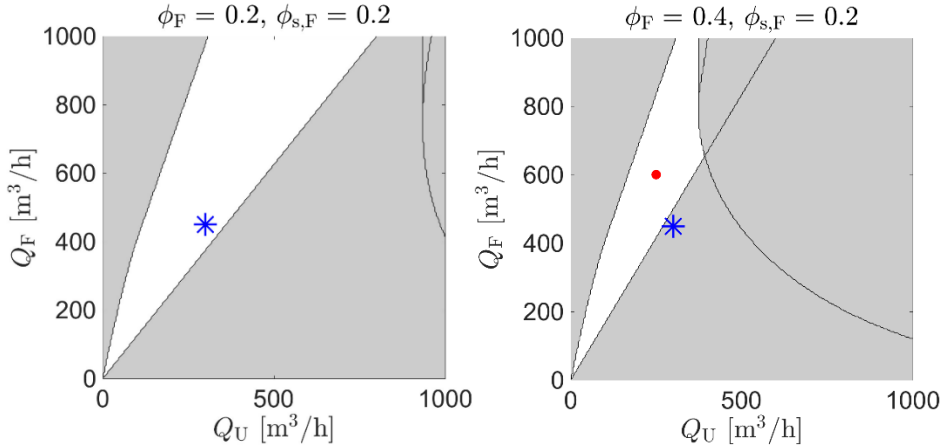

Figure 6 DAF thickening with sedimentation: Operating charts in two cases of feed volume fractions of aggregates ϕ_F and solids $\phi_{s,F}$. The blue asterisk is the first operating point and the red dot the one after the control action.

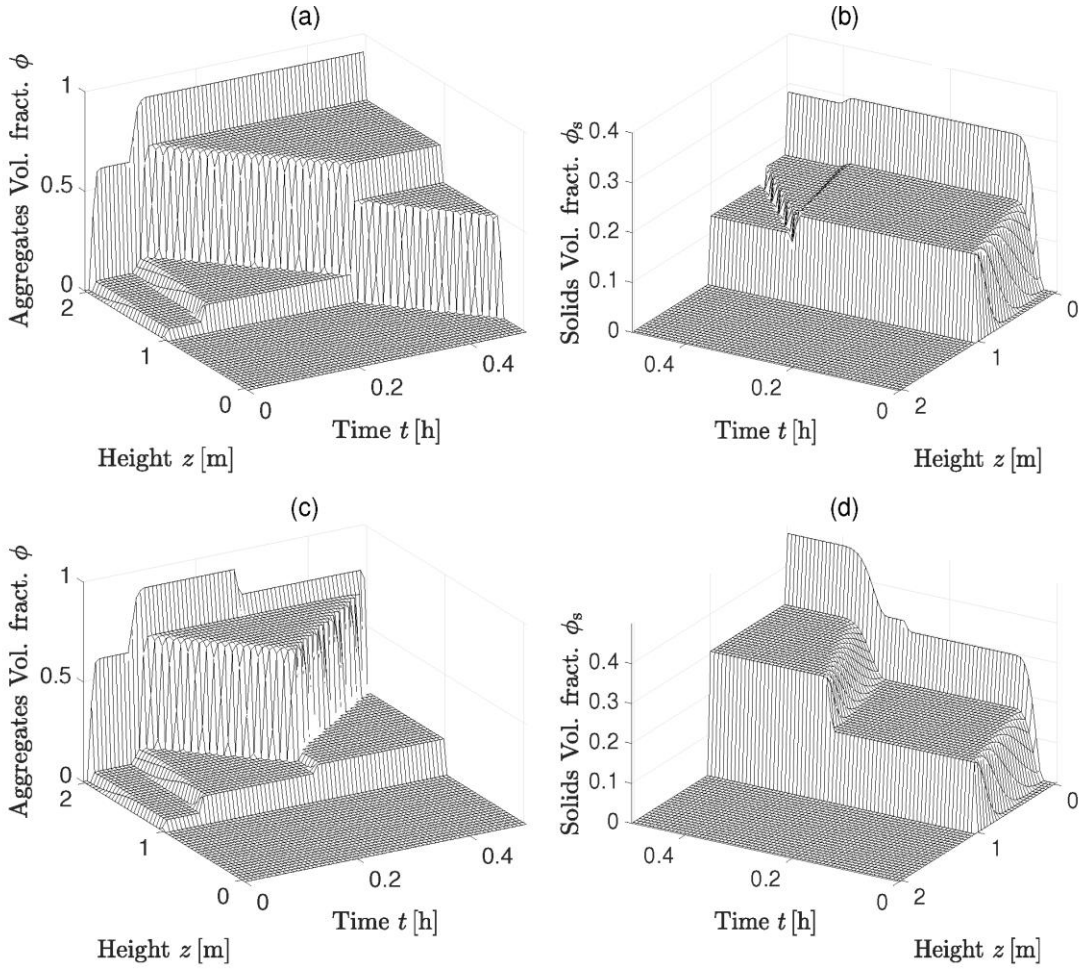

Figure 7 DAF thickening with sedimentation. The first row show a simulation of aggregates (a) and solids (b) volume fraction without control action. A layer of aggregates is built up and grows into the thickening zone below the feed level (zone 1). The second row (c, d) show a simulation with control action at $t = 0.27$ h $= 16.2$ min.

Conclusions

The 1D modelling of column flotation has for half a century been limited to steady-state situations utilizing the drift-flux theory. This can be seen as a special case of a general dynamic modelling with PDEs in 1D. Based on recent advances of mathematical research related to the theory and numerical analysis for hyperbolic PDEs with discontinuous flux functions, the three-phase flow of rising aggregates and settling particles in a fluid can be modelled and simulated with several inlets and outlets. The model is based on the simplifying assumption that the aggregation process has been completed before the mixture is fed into the vessel. In the future, we intend to include the more realistic case that aggregation may occur within the vessel as the bubbles rise. The aggregation process is difficult to model; see, e.g., Fukushi *et al*., (1995). Then at least one additional PDE has to be added keeping track of the level of aggregation of the bubbles as function of time and height. Other extensions are to include compression effects at high concentrations and take the hydrostatic pressure into account for tall flotation columns.

Acknowledgements

R.B. acknowledges support by Fondecyt project 1170473; CONICYT/PIA/Concurso Apoyo a Centros Científicos y Tecnológicos de Excelencia con Financiamiento Basal AFB170001; CRHIAM, Proyecto Conicyt/Fondap/15130015; and by the INRIA Associated Team ``Efficient numerical schemes for non-local transport phenomena'' (NOLOCO; 2018-2020). M.C.M. is supported by Spanish MINECO grant MTM2017-83942-P. Y.V. is supported by SENACYT (Panama).

References

Bratby, J. R., Ambrose, W. A. (1995). Design and control of flotation thickeners. *Water Sci. Tech*. 31 (3–4): 247–261.

Butler, R. C., Finger, R. E., Pitts, J. F. and Strutynski, B. (1997). Advantages of cothickening primary and secondary sludges in dissolved air flotation thickeners. *Water Environ. Res*. 69, 311–316.

Bürger, R., Diehl, S. and Martí, M. C. (2018). A conservation law with multiply discontinuous flux modelling a flotation column, *Networks Heterog. Media* 13, 339–371.

Bürger, R., Diehl, S. and Martí, M. C. (2019). A system of conservation laws with discontinuous flux modelling flotation with sedimentation. Preprint 2019-09, CI^{2}MA and Departamento de Ingeniería Matemática, Universidad de Concepción.

Bürger, R., Diehl S., Farås, S., Nopens I., and Torfs, E. (2013). A consistent modelling methodology for secondary settling tanks: A reliable numerical method. *Water Sci. Tech*. 68(1), 192–208.

Chung, T. H. and Kim, D. Y. (1997). Significance of pressure and recirculation in sludge thickening by dissolved air flotation, *Water Sci. Tech*. 36(12), 223–230.

Dickinson, J. E. and Galvin, K. P. (2014). Fluidized bed desliming in fine particle flotation – part I. *Chem. Eng. Sci*. 108, 283–298.

Diehl, S. (1996). A conservation law with point source and discontinuous flux function modelling continuous sedimentation. *SIAM J. Appl. Math*. 56, 388–419.

Finch, J. A. and Dobby, G. S. (1990). *Column Flotation*. Pergamon Press, London.

Fukushi, K., Tambo, N., Matsui, Y. (1995). A kinetic model for dissolved air flotation in water and wastewater treatment. *Water Sci. Tech*. 31 (3–4), 37–47.

Galvin, K. P. and Dickinson, J. E. (2014). Fluidized bed desliming in fine particle flotation – part II: Flotation of a model feed, *Chem. Eng. Sci*. 108, 299–309.

Haarhoff, J. and Bezuidenhout, E. (1999). Full-scale evaluation of activated sludge thickening by dissolved air flotation. *Water SA*, 25(2), 153–166.

Katz, W. J. and Geinopolos, A. (1967) Sludge thickening by dissolved-air flotation. *J. Water Pollution Control Federation*, 39(6), 946–957.

Karlsen, K. H., Mishra, S. and Risebro, N. H. (2009). Convergence of finite volume schemes for triangular systems of conservation laws. *Numer. Math*. 111, 559–589.

Reali, M., Patrizzi, L. J., Cordeiro, J. S. (2019). Comparison of thickening of sludges produces in two water treatment plants by using DAF and gravity. *Minerva* 2(2), 195–201.

Rubio, J., Souza, M. L. and Smith, R. W. (2002). Overview of flotation as a wastewater treatment technique, *Minerals Eng*. 15, 139–155.

Saththasivam, J., Loganathan, K. and Sarp, S. (2016). An overview of oil–water separation using gas flotation systems, *Chemosphere* 144, 671–680.

Wallis, G. B. (1969). *One-dimensional Two-phase Flow*. McGraw-Hill, New York, 281 pp.

Wang L. K., Shammas N. K., Selke W. A., Aulenbach D. B. (2007). Flotation Thickening. In: Wang L. K., Shammas N. K., Hung YT. (eds). *Biosolids Treatment Processes. Handbook of Environmental Engineering*, vol 6. Humana Press.